

# Specific Heat of the $\beta$ -Pyrochlore Oxide Superconductors $\text{CsOs}_2\text{O}_6$ and $\text{RbOs}_2\text{O}_6$

Zenji Hiroi\*, Shigeki Yonezawa, Takaki Muramatsu, Jun-Ichi Yamaura  
and Yuji Muraoka

*Institute for Solid State Physics, University of Tokyo, Kashiwa, Chiba 277-8581*

Two  $\beta$ -pyrochlore oxide superconductors,  $\text{CsOs}_2\text{O}_6$  and  $\text{RbOs}_2\text{O}_6$ , are studied thermodynamically by measuring specific heat on polycrystalline samples. It is found that a Sommerfeld coefficient  $\gamma$  is nearly equal,  $20 \text{ mJ/K}^2 \text{ mol Os}$ , in the two oxides with different superconducting transition temperatures;  $T_c = 3.3 \text{ K}$  and  $6.3 \text{ K}$ , respectively. This suggests that the density of states at the Fermi level is not a crucial parameter to determine the  $T_c$  of the  $\beta$ -pyrochlore oxide superconductors, which is incompatible with the general expectation for a conventional BCS-type superconductor. Anomalous lattice contributions to specific heat at low temperature are also reported, which may come from nearly localized phonon modes associated with the rattling of the alkali metal ions weakly bound in an oversized cage formed by  $\text{OsO}_6$  octahedra.

**KEYWORDS:** superconductivity,  $\beta$ -pyrochlore oxide,  $\text{CsOs}_2\text{O}_6$ ,  $\text{RbOs}_2\text{O}_6$ , specific heat, Sommerfeld coefficient, phonon

\*E-mail address: hiroi@issp.u-tokyo.ac.jp

## 1. Introduction

One of recent trends in the study of superconductivity is to search for a new superconductor with triangle-based lattices. The uniqueness of triangles is recognized, when one considers a localized spin on each lattice point interacting antiferromagnetically with the neighbours. Then, associated geometrical frustration may destroy long-range order and induce an unusual ground state such as a spin glass or a spin liquid.<sup>1)</sup> An interesting and untouched issue is to elucidate how this geometrical frustration influences the ground states of strongly correlated electron systems on triangle-based lattices, such as transition metal (TM) oxides, which lie between localized spin and itinerant electron systems. In particular, possible effects on superconducting ground states would be an attracting topic and have been studied extensively in several years.

The first TM oxide superconductor with a triangle-based lattice is probably  $\text{LiTi}_2\text{O}_4$  which was reported long time ago to become superconducting below  $T_c = 13.7 \text{ K}$ .<sup>2)</sup> It crystallizes in the spinel structure where a titanium ion with one half  $3d$  electron forms the pyrochlore lattice made of corner-sharing tetrahedra. The mechanism of the superconductivity has not yet been understood well, but may be described in the framework of the conventional Bardeen-Cooper-Schrieffer (BCS) the-

ory.<sup>3)</sup> Another class of transition metal oxides possessing the pyrochlore lattice is pyrochlore oxides with the general formula  $\text{A}_2\text{B}_2\text{O}_7$  or  $\text{A}_2\text{B}_2\text{O}_6\text{O}'$  with B a transition metal.<sup>4)</sup> About three years ago, superconductivity with  $T_c = 1.0 \text{ K}$  was found in  $\text{Cd}_2\text{Re}_2\text{O}_7$  for the first time in the family of pyrochlore oxides.<sup>5-7)</sup> Although the possibility of exotic superconductivity and the role of frustration on the mechanism have attracted a great deal of attention, it is now believed that the superconductivity is rather conventional.<sup>8, 9)</sup> Recently, the triangular lattice of  $\text{CoO}_2$  in  $\text{Na}_x\text{CoO}_2 \cdot y\text{H}_2\text{O}$  was rendered superconducting at  $T_c = 4 \sim 5 \text{ K}$ , although the mechanism still remains an open question.<sup>10)</sup>

Very recently, we found another pyrochlore-based superconductors  $\text{AOs}_2\text{O}_6$ , where A is a monovalent alkali metal like Cs,<sup>11)</sup> Rb,<sup>12)</sup> and K.<sup>13)</sup> The  $T_c$  is  $3.3 \text{ K}$ ,  $6.3 \text{ K}$ , and  $9.6 \text{ K}$ , respectively, much higher than in  $\text{Cd}_2\text{Re}_2\text{O}_7$ . The superconductivity of  $\text{RbOs}_2\text{O}_6$  was also reported by Kazakov and his coworkers.<sup>14)</sup> Because of apparent differences in the composition and crystal structure,  $\text{AOs}_2\text{O}_6$  is called the  $\beta$ -pyrochlore oxide, while  $\text{Cd}_2\text{Re}_2\text{O}_7$  is the  $\alpha$ -pyrochlore oxide.<sup>12)</sup> It is to be noted that the TM ions which are arranged on the pyrochlore lattice are in a five and a half valent state in the former, while in a pentavalent state in the latter. Consequently, there are formally one and a half  $5d$  electrons per TM ion in  $\text{AOs}_2\text{O}_6$ , while two  $5d$  electrons in  $\text{Cd}_2\text{Re}_2\text{O}_7$ . On one hand, a related  $\alpha$ -pyrochlore

oxide  $\text{Cd}_2\text{Os}_2\text{O}_7$  with three  $5d$  electrons exhibits a metal-to-insulator (MI) transition at 225 K on cooling.<sup>15, 16)</sup> This striking contrast in physical properties dependent on electron density illustrates rich physics involved in the  $5d$  TM pyrochlore oxides on the basis of electron correlations near the MI transition and possibly frustration on the pyrochlore lattice.

There have been a few experimental evidences to indicate the possibility of unconventional superconductivity realized in  $\text{AOs}_2\text{O}_6$ . One is a large upper critical field  $H_{c2}$  in  $\text{KOs}_2\text{O}_6$ .<sup>17)</sup> It was estimated to be 38 T by extrapolating lower field data, twice as large as Pauli's limit. The others are two resonance experiments:  $\mu\text{SR}$  experiments by Koda *et al.* on  $\text{KOs}_2\text{O}_6$  suggested the presence of an anisotropic order parameter,<sup>18)</sup> which is in contrast to the previous experimental results on  $\text{Cd}_2\text{Re}_2\text{O}_7$  revealing an isotropic gap.<sup>19)</sup> In NMR experiments on  $^{39}\text{K}$  and  $^{87}\text{Rb}$  nuclei, Arai *et al.* found a small peak in  $1/(T_1T)$  slightly below  $T_c$  for  $\text{RbOs}_2\text{O}_6$ , while no peaks for  $\text{KOs}_2\text{O}_6$ , which strongly suggests that unconventional superconductivity is realized, especially in  $\text{KOs}_2\text{O}_6$ .<sup>20)</sup> In contrast, there are a few reports insisting that the superconductivity of  $\text{RbOs}_2\text{O}_6$  is of conventional BCS type.<sup>21, 22)</sup> Generally speaking, it is always a hard work to determine the symmetry of Cooper pairs unambiguously in a new superconductor, and one needs accumulation of various, reliable experimental data as well as theoretical analyses. They are obviously not sufficient at the moment for the  $\beta$ -pyrochlore oxides.

Specific heat data would give an important clue to understanding the mechanism of superconductivity. However, no reliable data have been presented so far for the  $\beta$ -pyrochlore oxides. One of obstacles is poor quality of samples. Specific heat should be measured on a pure sample, because it is not a microscopic probe such as NMR but a bulk probe. Unfortunately, it has been difficult to prepare a single phase polycrystalline sample, because one has to deal with complicated reaction processes or avoid the toxicity of  $\text{OsO}_4$  which can be produced in the reaction process. Moreover, single crystal growth experiments have been unsuccessful. As a result, fundamental parameters necessary to describe the normal state, such as a Sommerfeld coefficient  $\gamma$ , have not yet been reported, except for the case of  $\text{RbOs}_2\text{O}_6$ : Bruhwilder *et al.* reported  $\gamma = 17 \text{ mJ/K}^2 \text{ mol Os}$  for  $\text{RbOs}_2\text{O}_6$  from their specific heat measurements using a polycrystalline sample.<sup>21)</sup> However, their sample contained a large non-superconducting fraction of more than 20%, as estimated from a residual  $\gamma$  value.

In this report, we present specific heat data for  $\text{CsOs}_2\text{O}_6$  and  $\text{RbOs}_2\text{O}_6$  which have been obtained

on well characterized polycrystalline samples consisting of two phases;  $\text{AOs}_2\text{O}_6$  and Os metal. The content of the Os metal had been determined by Rietveld analyses using powder X-ray diffraction data, and its contribution to specific heat was calculated and subtracted from raw data. As a result, we found nearly the same  $\gamma$  value of  $\gamma = 20 \text{ mJ/K}^2 \text{ mol Os}$  for the two oxides. In the case of  $\text{KOs}_2\text{O}_6$  we have not yet been successful to prepare such a two phase mixture to obtain a reliable specific heat data.

## 2. Experimental

Two polycrystalline samples were prepared for each oxide by solid state reaction from  $\text{A}_2\text{O}$  ( $\text{A} = \text{Cs}, \text{Rb}$ ) and  $\text{OsO}_2$  (Alfa Aesar) or Os metal by heating at 773 - 873 K for 24 h under controlled oxygen partial pressures.<sup>11, 12)</sup> All the products were composed of three phases, as examined by powder X-ray diffraction (XRD) experiments: The main phase was  $\text{AOs}_2\text{O}_6$ , and the minor ones were  $\text{AOsO}_4$  and Os metal. Although we had tried to reduce the amount of these minor phases in various conditions, it was unsuccessful probably due to slow reactions or partial decompositions. Fortunately,  $\text{AOsO}_4$  could be removed thoroughly from the sample by dissolving it in water. Thus, we obtained finally a two-phase mixed sample;  $\text{CsOs}_2\text{O}_6 + \text{Os}$  or  $\text{RbOs}_2\text{O}_6 + \text{Os}$ . In order to estimate the Os content in the samples, we carried out the Rietveld analyses of powder XRD patterns by using a software RIETAN2000 developed by Izumi.<sup>23)</sup> The XRD data were collected at room temperature over the  $2\theta$  range 10-120° on a rotating anode diffractometer with graphite-monochromated  $\text{Cu-K}\alpha$  radiation. It was found that the samples contained 10-30 wt% Os, and specific heat data were corrected using these values, as will be mentioned later. Independent of the coexisting Os content, the  $T_c$  determined by resistivity measurements was the same; 3.3 K and 6.3 K for Cs and Rb samples, respectively. Moreover, magnetic shielding fractions measured in a 10 Oe field were sufficiently large, ~ 100 % or more, though it was difficult to estimate actual superconducting volume fractions in the samples from them.

Specific heat measurements were performed by the heat-relaxation method in a temperature range between 0.4 K and 35 K and in a magnetic field up to 12 T in a Quantum Design Physical-Property-Measurement-System equipped with a  $^3\text{He}$  refrigerator. A thin plate-like pellet of 15 ~ 30 mg weight was attached to an alumina platform by a small amount of Apiezon N grease. In each measurement, heat capacity was obtained by fitting a heat relaxation curve recorded after a heat pulse giving a temperature rise of approximately 2%.

The fitting was done using the two-tau model which assumes two time constants,  $\tau_1$  and  $\tau_2$ . The  $\tau_1$  describes heat relaxation inside the sample and the  $\tau_2$  takes into account poor thermal attachment of the sample to the platform. The data at high temperature above 1 K could be well fitted by a single component, while at lower temperature the two-tau model gave a reasonable fitting: Typically,  $\tau_2 = \tau_1/1000$  at high temperature above 1 K and  $\tau_2 = \tau_1/100$  at the lowest temperature. The heat capacity of an addendum had been measured in a separate run without a sample, and was subtracted from the data. The measurements were done three times at each temperature with a scatter less than 1% at most.

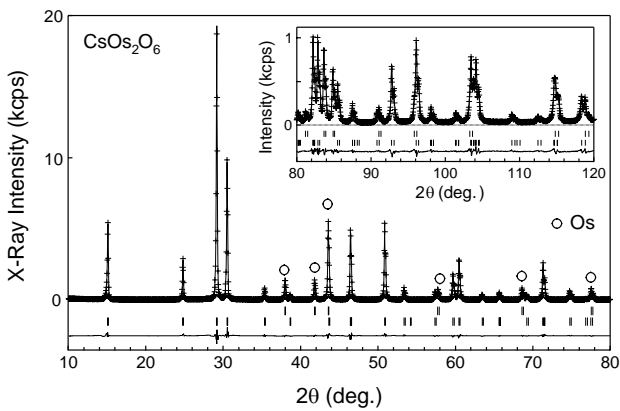


Fig. 1. X-ray diffraction pattern of  $\text{CsOs}_2\text{O}_6$  (sample #2) analyzed by the Rietveld method. Small crosses are experimental data, and a solid line is a fit to them calculated by assuming a mixture of  $\text{CsOs}_2\text{O}_6$  and Os. The peak positions from them are shown by short bars below the pattern. Peaks from Os are also marked with circles. The lowest line shows differences between experimental and calculated intensities.

Table I. Comparison of osmium metal content, a Sommerfeld coefficient  $\gamma$  and a coefficient of the  $T^5$  term in the lattice contributions  $\beta'$  for the four samples of  $\beta$ -pyrochlore oxide superconductors examined in the present study.

Sample	$\text{CsOs}_2\text{O}_6$		$\text{RbOs}_2\text{O}_6$	
	#1	#2	#1	#2
Os metal content (%)	16.4	18.4	26.2	11.5
$\gamma$ ( $\mu\text{J}/\text{K}^2 \text{ mol Os}$ )	20.0	19.5	20.2	21.7
$\beta'$ ( $\mu\text{J}/\text{K}^6 \text{ mol Os}$ )	7.2	8.7	5.0	17.5

### 3. Results and Discussion

#### 3.1 Subtraction of the Os metal contribution

First of all, Os content in the four samples was determined by the Rietveld analyses, and its contribution to specific heat was calculated. Figure 1 shows a typical result of Rietveld analyses performed on a sample  $\text{CsOs}_2\text{O}_6$  (#2). XRD intensity was calculated assuming the two-phase coexistence of  $\text{CsOs}_2\text{O}_6$  (cubic, space group  $Fd-3m$ ) and Os (hexagonal, space group  $P6_3/mmc$ ). Agreements between the experimental data and the calculations are fairly good with a low final  $R$  factor of  $R_{wp} = 7.1\%$ . The refined lattice constants are  $a = 1.01477(1)$  nm for  $\text{CsOs}_2\text{O}_6$ , and  $a = 0.27332(1)$  nm and  $c = 0.43182(1)$  nm for Os. More sophisticated structural refinements using a synchrotron radiation light source will be reported elsewhere.<sup>24)</sup> Here, it is important to note that there are no extra peaks from other impurity phases, confirming the two-phase mixture. The mass fraction of Os was determined to be 18.4% for this sample. Similar analyses on the rest of the samples lead us to the Os content listed in Table 1.

Next, we have estimated the heat capacity of Os metal present in each sample, and subtracted it from the raw data. Figure 2 shows typical data for  $\text{CsOs}_2\text{O}_6$  (#1), where the raw heat capacity data  $C_{\text{exp}}$  measured at magnetic fields of 0 and 5 T are plotted against temperature. It exhibits a hump below  $T_c = 3.3$  K and decreases to zero smoothly as  $T \rightarrow 0$  K. In contrast,  $T$ -linear behaviour is clearly observed at  $H = 5$  T without a hump, suggesting that superconductivity is suppressed completely by the field. The coefficient of the  $T$ -linear term is  $1.548 \mu\text{J}/\text{K}^2$ . This  $C_{\text{exp}}$  should be the sum of  $C(\text{CsOs}_2\text{O}_6)$  and  $C(\text{Os})$ . The Os content of this sample is 16.4%, which means that the weight of Os is 4.62 mg in the total sample weight of 28.20 mg. Using the Sommerfeld coefficient of Os from the literature ( $\gamma(\text{Os}) = 2.35 \text{ mJ}/\text{K}^2 \text{ mol}$ ), the electronic contribution of Os in the sample is decided to be  $0.0571 \mu\text{J}/\text{K}^2$ , which is only 3.7% of the total  $T$ -linear term. On one hand, the lattice part of coexisting Os is also ignorable in the Debye model with a Debye temperature  $\Theta_D = 500$  K; e.g.,  $0.025 \mu\text{J}/\text{K}$  at  $T = 4$  K. The total specific heat from Os is shown in Fig. 2, which is apparently much smaller than the raw data. Therefore, the correction of the raw data due to the coexistence of Os metal is rather small. However, specific heat per mol of  $\text{CsOs}_2\text{O}_6$  is increased significantly by about 20% after the correction, because the actual weight of  $\text{CsOs}_2\text{O}_6$  is reduced to 23.58 mg. Obviously, this is crucial to determine the right value of  $\gamma$ . All the specific heat data given hereafter have been corrected for coexisting Os metal.

Osmium metal becomes superconducting below  $T_c = 0.66$  K. Nevertheless, no anomaly is discernible near the  $T_c$  in Fig. 2. The associated jump in specific heat  $\Delta C$  at  $T_c$  expected from the BCS theory is  $1.43\gamma T_c$ , and is calculated to be  $0.054 \mu\text{J/K}$  in the present case, which corresponds to 27% of the raw data near the  $T_c$ . This may be too small to observe, or Os present in the sample may be nonsuperconducting owing to some reason. Anyway, the effect of possible superconducting transition of Os can be ignored.

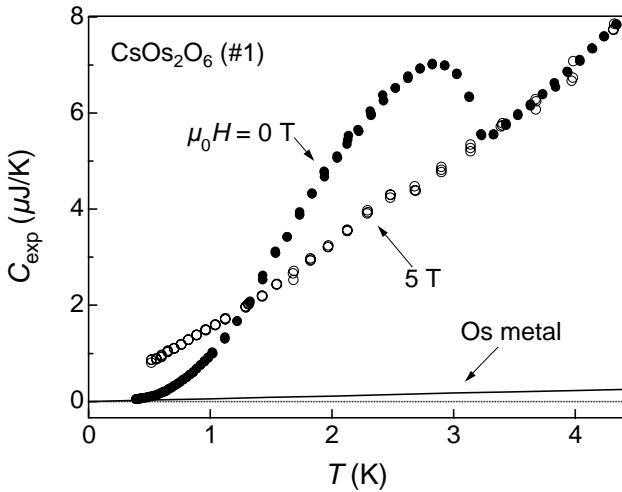


Fig. 2. Raw specific heat data of  $\text{CsOs}_2\text{O}_6$  (sample #1) measured at magnetic fields of zero (solid circles) and 5 T (open circles). Calculated contributions from coexisting Os metal (16.4 wt%) are shown with a solid line.

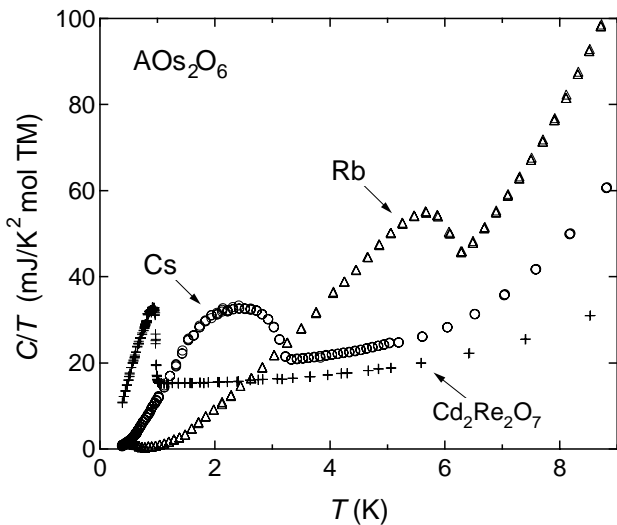


Fig. 3. Specific heat divided by temperature per one mol of transition metal (TM) atoms after the subtraction of Os contributions for  $\text{CsOs}_2\text{O}_6$  (#1) (circles),  $\text{RbOs}_2\text{O}_6$  (#1) (triangles), and  $\text{Cd}_2\text{Re}_2\text{O}_7$  (crosses).

Figure 3 shows the temperature dependence of specific heat divided by temperature per mol TM

after the above-mentioned correction for  $\text{CsOs}_2\text{O}_6$  (#1) and  $\text{RbOs}_2\text{O}_6$  (#1) as well as for  $\text{Cd}_2\text{Re}_2\text{O}_7$ . This may be the first specific heat data for  $\text{CsOs}_2\text{O}_6$ . For  $\text{RbOs}_2\text{O}_6$ , the present data shows a larger and sharper change at  $T_c$ , compared with our previous data,<sup>12)</sup> suggesting a better sample quality. The  $T_c$  defined as the edge of the hump is 3.3 K and 6.3 K, for Cs and Rb, respectively. Through the comparison to the data of  $\text{Cd}_2\text{Re}_2\text{O}_7$  taken by using a single crystal, it is clear that the superconducting transition of the two  $\beta$ -pyrochlore oxides is considerably broad for. This may be due to the polycrystalline form of the samples and also due to certain inhomogeneity present in the samples.

### 3.2 Specific heat of the lattice

Generally, the specific heat of a metallic compound consists of two components:  $C_e$  from conduction electrons and  $C_{ph}$  from phonons. In the low temperature limit,  $C_e = \gamma T$  with a Sommerfeld coefficient  $\gamma$ , and  $C_{ph} = \beta T^3$  in the Debye model assuming low-energy acoustic phonons. The specific heat of  $\alpha$ -pyrochlore  $\text{Cd}_2\text{Re}_2\text{O}_7$  is expressed certainly as  $\gamma T + \beta T^3$  below 3 K with  $\gamma = 15.1 \text{ mJ/K}^2 \text{ mol Re}$  and  $\beta = 0.111 \text{ mJ/K}^4 \text{ mol Re}$ .<sup>5)</sup> The Debye temperature  $\Theta_D$  is 458 K from the relation  $\alpha\Theta_D^3 = 1943.7N$ , where  $N$  is the number of atoms in the formula per Re. In other metallic pyrochlore oxides,  $\Theta_D = 300 \sim 450$  K was reported.<sup>4)</sup> It is considered in the Debye model that the deviation from the  $T^3$  law starts above  $T = \Theta_D/50$ .<sup>25)</sup>

Back to Fig. 3, the  $C/T$  of  $\text{AOs}_2\text{O}_6$  increases more rapidly with temperature than that of  $\text{Cd}_2\text{Re}_2\text{O}_7$ , suggesting a substantial difference in the phonon part between  $\alpha$  and  $\beta$ -pyrochlores. Moreover, the slope of  $\text{RbOs}_2\text{O}_6$  is significantly larger than that of  $\text{CsOs}_2\text{O}_6$ . Following the ordinary way, we have plotted the  $C/T$  against  $T^2$  in Fig. 4. In each compound the temperature dependence shows always a convex-downward curvature even at very low temperature, instead of a linear relation expected from the Debye model. Alternatively, we have plotted it against  $T^4$ , which shows apparently a linear relation in a wide temperature range. Therefore, the  $\beta$  is negligibly small compared with the  $\beta$  in the expression of  $C_{ph} = \beta T^3 + \beta T^5$  in this temperature range. The absence of the  $T^5$  term is also demonstrated in Fig. 5, where  $(C - \gamma T)/T^3$  is plotted. The  $\beta$  value decided from Fig. 4 is given in Table 1. In the logarithmic plot of  $(C - \gamma T)$  versus  $T$ , we found an apparent linear relation for  $T_c < T < 7 \sim 8$  K. From the slope a more accurate value for the power in the temperature dependence of  $C_{ph} \propto T^n$  could be obtained as  $n = 5.2$  (Cs) and 5.1 (Rb).

The  $T^3$  law is expected when only low-energy acoustic phonons with energy  $\hbar\omega$  proportional to

momentum transfer  $q$  are excited at low temperature. On one hand,  $C$  is proportional to  $T^{3/2}$  for  $\hbar\omega \propto q^2$  in the case of spin waves in ferromagnetic materials. In general,  $C$  is proportional to  $T^{3/n}$  for an excitation wave with a dispersion relation of  $\hbar\omega \propto q^n$  in the low temperature limit. Thus, the present  $T^5$  behaviour could be interpreted qualitatively by assuming unusual unharmonic phonons with  $\hbar\omega \propto q^{3/5}$ .

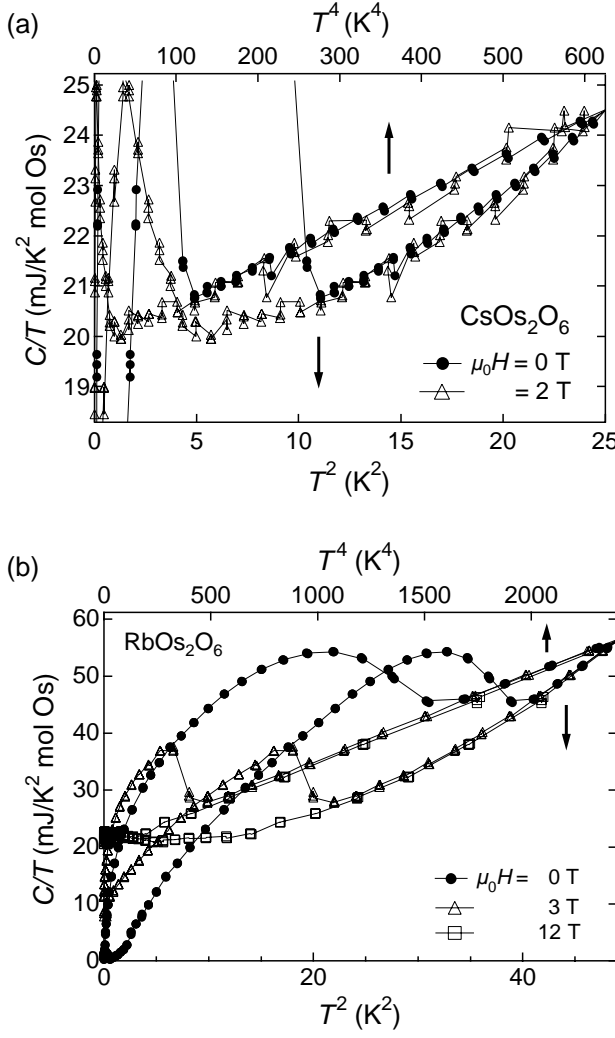


Fig. 4. Specific heat divided by temperature plotted twice against  $T^2$  (bottom axis) and  $T^4$  (top axis), below  $T = 5$  K for  $\text{CsOs}_2\text{O}_6$  (#1) (a) and below  $T = 7$  K for  $\text{RbOs}_2\text{O}_6$  (#1) (b). Data taken at zero field (solid circles) and at fields (open marks) are shown.

In order to discuss on the lattice specific heat at high temperature,  $(C-\gamma T)/T^3$  is plotted against  $T$  in Fig. 5. That of  $\text{Cd}_2\text{Re}_2\text{O}_7$  approaches to a finite value of  $0.11 \text{ mJ/K}^4 \text{ mol Re}$  as  $T \rightarrow 0$  K, while those of  $\text{AOs}_2\text{O}_6$  apparently go to zero or a much smaller value, implying that the  $T^3$  term is missing. It is also to be noted that there are large enhance-

ments in  $(C-\gamma T)/T^3$  at high temperature. This can be explained by assuming dominant contributions from Einstein modes: The Debye model predicts that the deviation from the  $T^3$  law at high temperature occurs so as to reduce the power, and thus  $(C-\gamma T)/T^3$  should decrease with increasing temperature. In contrast, the specific heat of the Einstein model is given by

$$C_E = 3R \left( \frac{\Theta_E}{T} \right)^2 \frac{\exp(\Theta_E/T)}{[\exp(\Theta_E/T)-1]^2},$$

where  $R$  is the gas constant and  $\Theta_E$  is the Einstein temperature. Thus, the  $C_E/T^3$  should increase rapidly at first as  $T$  increases, as observed in Fig. 5.

Similar enhancements in  $(C-\gamma T)/T^3$  at high temperature have been reported in various one-dimensional organic conductors like  $(\text{TMTSF})_2\text{PF}_6$  with a spin-density-wave (SDW) ground state, and are attributed to the coexistence of a single Debye mode and double Einstein modes.<sup>26)</sup> By analogy with this, here we have taken into account only the latter contribution and fitted the data at high temperature above 10 K as shown in Fig. 5. The  $C_E$  is assumed to be  $aC_{E1} + bC_{E2}$ , with two Einstein temperatures,  $\Theta_{E1}$  and  $\Theta_{E2}$ , as free parameters. The results of fitting are satisfactory as shown in Fig. 5, with  $(a, \Theta_{E1}/\text{K}, b, \Theta_{E2}/\text{K}) = (0.542, 69.7, 1.00, 173)$  and  $(0.553, 61.4, 1.03, 138)$  for the Cs and Rb samples, respectively.

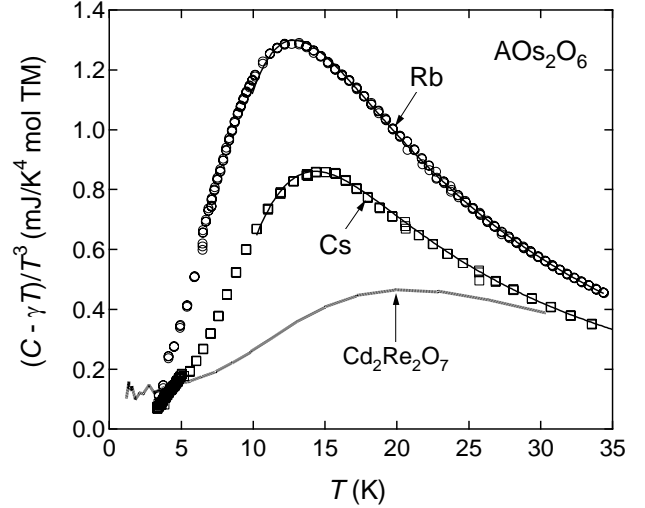


Fig. 5. Comparison of the temperature dependences of  $(C-\gamma T)/T^3$  for  $\text{CsOs}_2\text{O}_6$  (squares),  $\text{RbOs}_2\text{O}_6$  (circles), and  $\text{Cd}_2\text{Re}_2\text{O}_7$  (broken line). Data taken at  $H = 2$  T and 12 T are added to the zero-field data for  $A = \text{Cs}$  and  $\text{Rb}$ , respectively. The data below  $T_c$  are omitted for clarity. The solid lines on the data points are fits to the model described in the text.

A prominent and common feature on the crystal structure of the  $\beta$ -pyrochlore oxides is that an alkali metal ion lies in a cage made of  $\text{OsO}_6$  octahedra,

replacing a much larger  $A_4O'$  tetrahedron in the  $\alpha$ -pyrochlore oxides  $A_2B_2O_6O'$ . Thus, the cage is too large even for a large alkali metal ion. Our recent structural refinements by the Rietveld method gave in fact unusually large isotropic displacement factors  $B$  in the Debye-Waller temperature factor for the alkaline metal ions;  $B = 2.0 \text{ \AA}^2$  for Cs and  $B = 3.2 \text{ \AA}^2$  for Rb.<sup>24)</sup> Note that the  $B$  is larger for smaller ions. This may be associated with the 'rattling' behaviour of the alkali metal ions in the cage, similar as reported in filled skutterudite compounds with a large thermoelectric efficiency.<sup>27)</sup> In cubic filled skutterudite antimonides with the formula  $RM_4Sb_{12}$ , where R is a rare-earth element and M is a transition metal, the R ion is weakly bound in an oversized atomic cage formed by the other atoms. Its presence causes a dramatic reduction in thermal conductivity and enhances thermoelectric efficiency. Two localized, incoherent vibrational modes with  $\Theta_E = 70 \text{ K}$  and  $200 \text{ K}$  were found in  $La_{0.9}Fe_3CoSb_{12}$  by specific heat measurements.<sup>28)</sup> Therefore, it is plausible to ascribe the two Einstein modes with  $\Theta_{E1} \approx 70$  (60) K and  $\Theta_{E1} \approx 170$  (140) K found in the Cs(Rb)  $\beta$ -pyrochlores to the rattling of the alkali metal ions. It would be interesting to measure the thermal conductivity of the  $\beta$ -pyrochlores in order to examine whether these localized modes reduce it, as in the case of the skutterudites. We would expect in this scenario larger rattling for K in  $KOs_2O_6$ , which will be clarified in future experiments.

The rattling modes are considered to be nearly localized modes with dispersionless excitations. However, completely localized modes such as in molecules should not exist in solids because of strong interactions between constituent atoms. Therefore, the rattling modes in the present compound must exhibit a certain dispersion at a low- $\omega$  and low- $q$  region which is to be continued to a nearly flat  $q$  dependence of  $\omega$  at a high- $\omega$  and high- $q$  region. It is plausible that such phonons possess a large unharmonicity characterized by an unusual dispersion relation of  $\hbar\omega \propto q^n$  with  $n < 1$ . The  $T^5$  behaviour observed below  $7 \sim 8 \text{ K}$  in the present study implies that  $\hbar\omega$  increases first as  $\hbar\omega \propto q^{3/5}$ . As a result, the observed unusual features of the lattice specific heat in the  $\beta$  pyrochlores can be explained qualitatively by assuming nearly localized rattling modes of the A atoms. Relation between the superconductivity and the rattling modes is an intriguing problem to be studied in the future.

### 3.3 Sommerfeld coefficient

The Sommerfeld coefficient  $\gamma$  was determined from the linear extrapolation of the  $C/T$  vs.  $T^4$  plot in Fig. 4. As listed in Table 1, it is 20.0 and 20.2

$\text{mJ/K}^2 \text{ mol Os}$  for the Cs and Rb samples, respectively. In order to check possible uncertainty arising from the subtraction of Os contributions, we carried out the same analyses on another sample with a different Os content for each compound. The  $\gamma$  value of the second sample is 19.5 and  $21.7 \text{ mJ/K}^2 \text{ mol Os}$  for samples Cs(#2) and Rb(#2), respectively, as shown in Table 1. The  $\gamma$  value of Rb(#2) is slightly larger than that of Rb(#1), but we take the latter as reliable, because the superconducting transition of Rb(#2) is considerably broad, compared with Rb(#1) (Fig. 7). Thus, we conclude that  $\gamma$  is nearly equal between the two compounds in spite of the large difference in  $T_c$ . This means that the change of  $T_c$  in the  $\beta$ -pyrochlores can not be ascribed to the change in DOS at the Fermi level,  $N(E_F)$ , of conduction electrons, which is proportional to  $\gamma$ .

Let us discuss briefly on the  $T_c$  in terms of the weak coupling BCS model. The  $T_c$  is often given by the equation,<sup>29)</sup>

$$T_c = \hbar\omega_{\text{ph}} \exp\left(-\frac{1}{VN(E_F)}\right),$$

where  $\omega_{\text{ph}}$  is the frequency of the relevant phonons and  $V$  is the electron-phonon coupling strength. If  $V$  and  $\omega_{\text{ph}}$  are assumed to be constant, the difference in  $N(E_F)$  for the two  $T_c$  values is given by

$$\frac{N'(E_F)}{N(E_F)} = \frac{\log(T_c/\omega_{\text{ph}})}{\log(T_c'/\omega_{\text{ph}})}.$$

Then, giving  $T_c = 3.3 \text{ K}$  and  $T_c' = 6.3 \text{ K}$  should result in  $N'/N = 1.15$  (1.23) in the case of  $\omega_{\text{ph}} = 500 \text{ K}$  (100 K). This estimation implies that the rise in  $N(E_F)$  by about 20% would be required to explain the increase in  $T_c$  from the Cs to Rb compounds. However, the observed difference in  $\gamma$  is significantly smaller than expected from the above estimation, suggesting that  $\omega_{\text{ph}}$  or  $V$  can be a variable. It happens in a similar alkaline metal substituted fullerene superconductor,  $A_3C_{60}$ , that the rise in  $T_c$  from 19.3 K ( $A = K$ ) to 29.3 K ( $A = Rb$ ) is well explained by the increase in  $N(E_F)$ .<sup>30)</sup> It is also to be noted that  $T_c$  is increased from  $A = K$  to Rb with expansion of the lattice in  $A_3C_{60}$ , as expected for a conventional BCS-type superconductor, while in the present system  $T_c$  is decreased with increasing the lattice volume from  $A = K$  to Cs. Moreover, very recent high-pressure experiments by Muramatsu *et al.* revealed a common feature on the pressure dependence of  $T_c$  for all the  $\beta$ -pyrochlore superconductors, where the  $T_c$  first increases with physical pressure, tends to saturate and decreases at higher pressure, and finally disappears above a critical pressure, *e.g.*,  $\sim 7 \text{ GPa}$  for  $RbOs_2O_6$ .<sup>31,32)</sup> It would be important to decide which parameter is relevant to these large changes in  $T_c$  under chemical

and physical pressures. From the present study, we can say that the DOS at the Fermi level may not be a crucial one.

Band structure calculations have already been performed by Saniz and co-workers for  $\text{KO}_{\text{Os}_2}\text{O}_6$ <sup>33)</sup> and by Harima for all the members of  $\beta$ -pyrochlores.<sup>34)</sup> According to them,  $\beta$ -pyrochlores commonly possess a semimetallic band structure as in  $\alpha$ -pyrochlore  $\text{Cd}_2\text{Re}_2\text{O}_7$ , but with much larger carrier density. There is a manifold of twelve branches in the vicinity of the Fermi level with a bandwidth of 3 eV, which come from strongly hybridized Os-5d and O-2p states. An important feature on the Fermi surface is the existence of octahedrally-shaped, thin shell-like sheets centered at the  $\Gamma$  point, which must give rise to strong nesting.<sup>34)</sup> Calculated  $\gamma$  values are 5.78 mJ/K<sup>2</sup> mol Os for  $\text{KO}_{\text{Os}_2}\text{O}_6$ <sup>33)</sup> and 4.8 ~ 5.6 mJ/K<sup>2</sup> mol Os for  $\text{AO}_{\text{Os}_2}\text{O}_6$ , slightly decreasing from Cs to K.<sup>34)</sup> Therefore, our experimental value of  $\gamma_{\text{exp}} = 20$  mJ/K<sup>2</sup> mol Os means a large specific heat mass enhancement of  $\gamma_{\text{exp}}/\gamma_{\text{cal}} \sim 4$  for A = Cs and Rb. The origin may be attributed to strong electron-phonon couplings or spin fluctuations associated with a SDW instability arising from the Fermi surface nesting.

### 3.4 Superconducting transition

Electronic contributions in specific heat after subtraction of the lattice part are shown in Fig. 6.  $C_e/T$  seems to decrease toward zero as  $T$  approaches zero in  $\text{CsOs}_2\text{O}_6$  (#1), indicating that residual  $\gamma$  ( $\gamma_{\text{res}}$ ) is almost absent and thus whole the sample becomes superconducting. Extrapolating  $C_e/T$  appropriately down to  $T = 0$  K, we obtained exact entropy balance between the experimental curve at  $H = 0$  and the line of  $C_e/T = \gamma$ , justifying the way of estimation of the lattice term and  $\gamma$ . In contrast, the superconducting transition of the second sample of  $\text{CsOs}_2\text{O}_6$  is a little broader than the first one, and the height of the hump is lower. Moreover, there is a residual  $\gamma$  corresponding to about 10% of the total  $\gamma$  of the normal state. On the other hand, the  $C_e/T$  of  $\text{RbOs}_2\text{O}_6$  (#1) measured at zero field seems to go to zero at low temperature, but finally exhibits an upturn below 0.7 K. Thus, the  $\gamma_{\text{res}}$  may be zero, but the sample must contain some defects inducing a Schottky-type specific heat, though the origin is not known. The second sample of  $\text{RbOs}_2\text{O}_6$  shows a broader superconducting transition with  $\gamma_{\text{res}} \sim 0$  and a similar upturn at low temperature.

Under magnetic fields, the hump shifts systematically to lower temperatures in each sample, as shown in Fig. 7 for  $\text{CsOs}_2\text{O}_6$  (#1) and  $\text{RbOs}_2\text{O}_6$  (#1). It is worthy of notice that the transition tends to become abrupt at certain fields, about 1 T for  $\text{CsOs}_2\text{O}_6$

and 3 T for  $\text{RbOs}_2\text{O}_6$ , and then broadened again at higher fields. This behaviour may not be explained by assuming a uniform distribution in  $T_c$  or  $H_{c2}$ , but by assuming that the sample contains a small portion with lower  $T_c$ 's and much smaller  $H_{c2}$ 's than the bulk. It is likely that the surface of particles is the place for that. The hump in  $C_e/T$  almost disappears at  $H = 5$  T in  $\text{CsOs}_2\text{O}_6$ , in good agreement with  $H_{c2} = 5.5$  T determined by resistivity measurements. In  $\text{RbOs}_2\text{O}_6$ , a trace of the hump seems to survive even at  $H = 12$  T, which is lower than  $H_{c2} = 15$  T estimated by resistivity measurements. This is in contrast to the previous report on  $\text{RbOs}_2\text{O}_6$  where a hump in specific heat disappeared completely at  $H = 12$  T, and  $H_{c2}$  was determined to be 6 T from specific heat data.<sup>21)</sup>

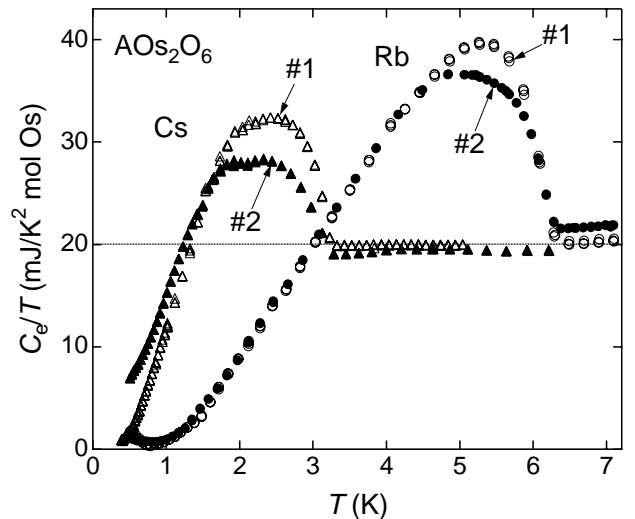


Fig. 6. Comparison of superconducting transitions observed in specific heat under zero field for the four samples.

Generally, specific heat data provide us with valuable information on the mechanism of superconductivity, because the shape of a superconducting transition observed in specific heat is determined by the formation of a gap at the Fermi surface and thus contains information on the anisotropy or symmetry of the gap. Especially important are the magnitude of the jump  $\Delta C_e$  at  $T_c$  and how  $C_e$  goes to zero at low temperature. Although the quality of the samples used in the present study seems to be rather poor, we will discuss on them briefly below.

Figure 8 compares the specific heat divided by  $\gamma T$  as a function of reduced temperature  $T/T_c$  of the present  $\beta$ -pyrochlores with those of a single crystal of  $\text{Cd}_2\text{Re}_2\text{O}_7$  and a polycrystal of  $\text{LiTi}_2\text{O}_4$ .<sup>35)</sup>  $\text{LiTi}_2\text{O}_4$  shows a sharp transition with a large jump  $\Delta C_e/\gamma T_c = 1.44$ , which is very close to 1.43 expected from the BCS theory in

the case of an isotropic gap opening on a spherical Fermi surface. On the other hand, the jump in  $\text{Cd}_2\text{Re}_2\text{O}_7$  is apparently smaller,  $\Delta C_e/\gamma T_c = 1.15$ , with keeping the transition sharp as well, suggesting a small anisotropy. In contrast, the jumps of the two  $\beta$ -pyrochlores are considerably smaller than the others. This is partly due to possible distributions in  $T_c$  in the samples. However, the jump would not exceed that of  $\text{Cd}_2\text{Re}_2\text{O}_7$ , even if one takes into account that possibility, which would push entropy (area below the  $C_e/\gamma T$  curve) at low temperature to higher temperature close to  $T_c$ . Concerning low temperature behaviour, we could fit the data of  $\text{CsOs}_2\text{O}_6$  by assuming either a power-law or an exponential temperature dependence. The former yielded  $n = 4.2$  in the expression  $C_e \propto T^n$ , and the latter did  $\Delta_0 = 4.4$  K in  $C_e \propto T^{-1.5} \exp(-\Delta_0/T)$ . In general arguments,  $n = 2$  and 3 for an anisotropic gap with line nodes and point nodes, respectively, and  $\Delta_0 = 5.8$  K for an isotropic gap with  $2\Delta_0/k_B T_c = 3.53$ . In the case of  $\text{RbOs}_2\text{O}_6$ , it was difficult to fit the data reasonably, because of the existence of the low-temperature upturn. Anyway, samples with better quality are required to discuss in more detail. On the gap symmetry, the NMR measurements indicated an isotropic gap with  $\Delta_0 = 1.8$  K ( $2\Delta_0/k_B T_c = 3.6$ ) for  $\text{Cd}_2\text{Re}_2\text{O}_7$ ,<sup>36)</sup> while suggested an anisotropic gap from the observed power-law temperature dependences in  $1/T_1$  with  $n = 3.6$  and 4.3 for  $\text{RbOs}_2\text{O}_6$  and  $\text{KO}_2\text{O}_6$ , respectively.<sup>20)</sup>

The origin of the observed broad transitions is not clear. Certain inhomogeneity present in the samples could be the candidate. We did not detect vacancies at the A site within our experimental errors, *i.e.*,  $\sim 1\%$ , in our Rietveld analyses.<sup>24)</sup> Moreover, it may not be plausible to assume the existence of oxygen vacancies from the crystal chemistry point of view. The fact that the  $T_c$  did not change from sample to sample, depending on the preparation conditions like starting metal compositions or oxygen partial pressures, suggests that uniform nonstoichiometry does not occur. It may be possible, nevertheless, that a very small amount of A-site vacancies exist and distribute inhomogeneously, for example near the surface of grains. On one hand, no structural deformations have been detected down to helium temperature by XRD and NMR measurements, the latter of which must be very sensitive to the change in local symmetry and

in fact found a cubic-to-tetragonal transition in  $\text{Cd}_2\text{Re}_2\text{O}_7$ .<sup>36)</sup>

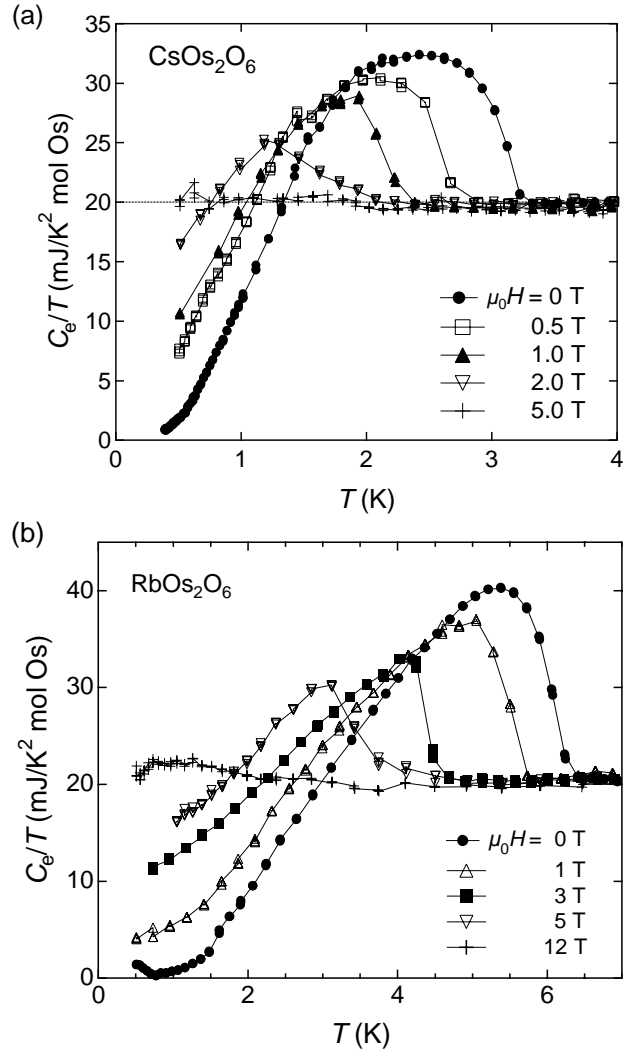


Fig. 7. Electronic specific heat  $C_e$  after the subtraction of lattice contributions measured at zero and various fields for  $\text{CsOs}_2\text{O}_6$  (#1) (a) and  $\text{RbOs}_2\text{O}_6$  (#1) (b).

Finally, we will make some comments about the previous report on specific heat measurements for  $\text{RbOs}_2\text{O}_6$ .<sup>21)</sup> They prepared a polycrystalline sample by removing  $\text{RbOsO}_4$  and obtained that  $\gamma = 17 \text{ mJ/K}^2 \text{ mol Os}$ . However, a large  $\gamma_{\text{res}}$  more than 20% was contained, which must come from a nonsuperconducting part in the sample. Moreover, they reported a large  $\beta T^3$  term below 4 K with  $\beta = 0.7 \text{ mJ/K}^4 \text{ mol Os}$ , which is missing in our experiments. They insisted a BCS-type superconductivity from the exponential temperature dependence of  $C$  after subtraction of contributions from the nonsuperconducting part. These marked differences in  $\gamma$  and  $\beta$  between their and our results may be ascribed to the difference in samples. We believe that the quality of our samples is better than theirs, and thus more

reliable specific heat data have been obtained in the present study. Although we carefully prepared and characterized our samples, still some problems have been left, such as broadening of the transition. It is necessary to obtain a better sample to clarify the essence of superconductivity in the  $\beta$ -pyrochlore oxides.

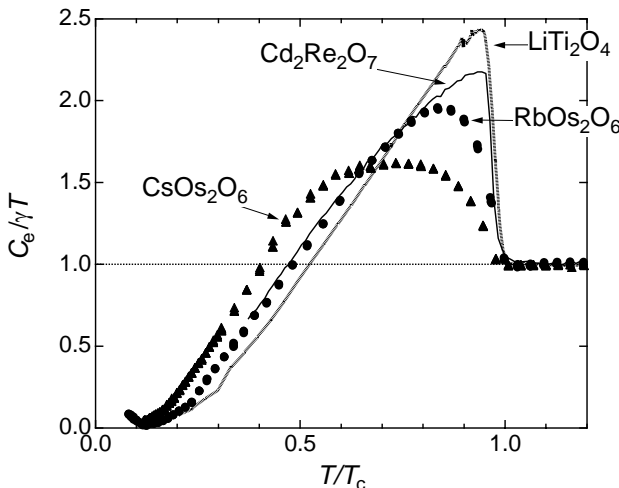


Fig. 8. Comparison of  $C_e$  divided by  $\gamma T$  versus  $T/T_c$  for  $\text{CsOs}_2\text{O}_6$  (triangles),  $\text{RbOs}_2\text{O}_6$  (circles),  $\text{Cd}_2\text{Re}_2\text{O}_7$  (solid line), and  $\text{LiTi}_2\text{O}_4$  (broken line). A single crystal is used for  $\text{Cd}_2\text{Re}_2\text{O}_7$ , and polycrystalline samples for the others. The sample of  $\text{LiTi}_2\text{O}_4$  was prepared by Isobe at ISSP.  $T_c$  (K) and  $\gamma$  (mJ/K<sup>2</sup> mol TM) is (3.3, 20.0), (6.3, 20.3), (1.0, 15.1), and (12.4, 8.3), respectively.

## 4. Conclusions

The specific heat data of the two  $\beta$ -pyrochlore oxide superconductors,  $\text{CsOs}_2\text{O}_6$  and  $\text{RbOs}_2\text{O}_6$ , are presented. It is found that a Sommerfeld coefficient  $\gamma$  is almost the same,  $\gamma = 20 \text{ mJ/K}^2 \text{ mol Os}$ , in the two compounds with different  $T_c$ 's. This implies that the DOS at the Fermi level is not a crucial parameter to determine the  $T_c$ , suggesting an unconventional mechanism of superconductivity. Anomalous lattice contributions are also found, which may come from the rattling of the A cations in the  $\beta$ -pyrochlore structure.

## Acknowledgments

We are grateful to K. Ueda, M. Takigawa and H. Harima for enlightening discussions. Z.H. thanks M. Isobe for providing us with a polycrystalline sample of  $\text{LiTi}_2\text{O}_4$ . This research was supported by a Grant-in-Aid for Scientific Research B (16340101) provided by the Ministry of Education, Culture, Sports, Science and Technology, Japan.

reliable specific heat data have been obtained in the present study. Although we carefully prepared and characterized our samples, still some problems have been left, such as broadening of the transition. It is necessary to obtain a better sample to clarify the essence of superconductivity in the  $\beta$ -pyrochlore oxides.

Fig. 8. Comparison of  $C_e$  divided by  $\gamma T$  versus  $T/T_c$  for  $\text{CsOs}_2\text{O}_6$  (triangles),  $\text{RbOs}_2\text{O}_6$  (circles),  $\text{Cd}_2\text{Re}_2\text{O}_7$  (solid line), and  $\text{LiTi}_2\text{O}_4$  (broken line). A single crystal is used for  $\text{Cd}_2\text{Re}_2\text{O}_7$ , and polycrystalline samples for the others. The sample of  $\text{LiTi}_2\text{O}_4$  was prepared by Isobe at ISSP.  $T_c$  (K) and  $\gamma$  (mJ/K<sup>2</sup> mol TM) is (3.3, 20.0), (6.3, 20.3), (1.0, 15.1), and (12.4, 8.3), respectively.

## 4. Conclusions

The specific heat data of the two  $\beta$ -pyrochlore oxide superconductors,  $\text{CsOs}_2\text{O}_6$  and  $\text{RbOs}_2\text{O}_6$ , are presented. It is found that a Sommerfeld coefficient  $\gamma$  is almost the same,  $\gamma = 20$  mJ/K<sup>2</sup> mol Os, in the two compounds with different  $T_c$ 's. This implies that the DOS at the Fermi level is not a crucial parameter to determine the  $T_c$ , suggesting an unconventional mechanism of superconductivity. Anomalous lattice contributions are also found, which may come from the rattling of the A cations in the  $\beta$ -pyrochlore structure.

## Acknowledgments

We are grateful to K. Ueda, M. Takigawa and H. Harima for enlightening discussions. Z.H. thanks M. Isobe for providing us with a polycrystalline sample of  $\text{LiTi}_2\text{O}_4$ . This research was supported by a Grant-in-Aid for Scientific Research B (16340101) provided by the Ministry of Education, Culture, Sports, Science and Technology, Japan.

1) A. P. Ramirez: *Annu. Rev. Mater. Sci.* **24** (1994) 453.  
 2) D. C. Johnston: *J. Low Temp. Phys.* **25** (1976) 145.  
 3) S. Foner and J. E.J. McNiff: *Solid State Commun.* **20** (1976) 995.  
 4) M. A. Subramanian, G. Aravamudan and G. V. S. Rao: *Prog. Solid State Chem.* **15** (1983) 55.  
 5) M. Hanawa, Y. Muraoka, T. Tayama, T. Sakakibara, J. Yamaura and Z. Hiroi: *Phys. Rev. Lett.* **87** (2001) 187001.  
 6) R. Jin, J. He, S. McCall, C. S. Alexander, F. Drymiotis and D. Mandrus: *Phys. Rev. B* **64** (2001) 180503.  
 7) H. Sakai, K. Yoshimura, H. Ohno, H. Kato, S. Kambe, R. E. Walstedt, T. D. Matsuda, Y. Haga and Y. Onuki: *J. Phys.: Condens. Matter* **13** (2001) L785.  
 8) O. Vyaselev, K. Arai, K. Kobayashi, J. Yamazaki, K. Kodama, M. Takigawa, M. Hanawa and Z. Hiroi: *Phys. Rev. Lett.* **89** (2002) 017001.  
 9) Z. Hiroi and M. Hanawa: *J. Phys. Chem. Solids* **63** (2002) 1021.  
 10) K. Takada, H. Sakurai, E. Takayama-Muromachi, F. Izumi, R. A. Dilanian and T. Sasaki: *Nature* **422** (2003) 53.  
 11) S. Yonezawa, Y. Muraoka and Z. Hiroi: *J. Phys. Soc. Jpn.* **73** (2004) 1655.  
 12) S. Yonezawa, Y. Muraoka, Y. Matsushita and Z. Hiroi: *J. Phys. Soc. Jpn.* **73** (2004) 819.  
 13) S. Yonezawa, Y. Muraoka, Y. Matsushita and Z. Hiroi: *J. Phys.: Condens. Matter* **16** (2004) L9.  
 14) S. M. Kazakov, N. D. Zhigadlo, M. Bruhwilder, B. Batlogg and J. Karpinski: *Supercond. Sci. Technol.* **17** (2004) 1169.  
 15) A. W. Sleight, J. L. Gilson, J. F. Weiher and W. Bindloss: *Solid State Commun.* **14** (1974) 357.  
 16) D. Mandrus, J. R. Thompson, R. Gaal, L. Forro, J. C. Bryan, B. C. Chakoumakos, L. M. Woods, B. C. Sales, R. S. Fishman and V. Keppens: *Phys. Rev. B* **63** (2001) 195104.  
 17) Z. Hiroi, S. Yonezawa and Y. Muraoka: *J. Phys. Soc. Jpn.* **73** (2004) 1651.  
 18) A. Koda, W. Higemoto, K. Ohishi, S. R. Saha, R. Kadono, S. Yonezawa, Y. Muraoka and Z. Hiroi: *cond-mat/0402400*.  
 19) R. Kadono, W. Higemoto, A. Koda, Y. Kawasaki, M. Hanawa and Z. Hiroi: *J. Phys. Soc. Jpn.* **71** (2002) 709.  
 20) K. Arai, J. Kikuchi, K. Kodama, M. Takigawa, S. Yonezawa, Y. Muraoka and Z. Hiroi: *cond-mat/0411460*.  
 21) M. Bruhwilder, S. M. Kazakov, N. D. Zhigadlo, J. Karpinski and B. Batlogg: *Phys. Rev. B* **70** (2004) 020503R.  
 22) R. Khasanov, D. G. Eshchenko, J. Karpinski, S. M. Kazakov, N. D. Zhigadlo, R. Brusch, D. Gavillet and H. Keller: *Phys. Rev. Lett.* **93** (2004) 157004.  
 23) F. Izumi: *The Rietveld Method*, ed. R. A. Young (Oxford Univ. Press, Oxford, 1993) p. 236.  
 24) S. Yonezawa, submitted to *Solid State Sciences*.  
 25) C. Kittel: *Introduction to solid state physics* (John Wiley & Sons, New York, 1976).  
 26) H. Yang, J. C. Lasjaunias and P. Monceau: *J. Phys.: Condens. Matter* **11** (1999) 5083.  
 27) B. C. Sales, D. Mandrus and R. K. Williams: *Science* **272** (1996) 1325.  
 28) V. Keppens, D. Mandrus, B. C. Sales, B. C. Chakoumakos, P. Dai, R. Coldea, M. B. Maple, D. A.

Gajewski, E. J. Freeman and S. Bennington: *Nature* **395** (1998) 876.

29) M. Tinkham: *Introduction to superconductivity* (Dover Publications, inc., New York, 1996).

30) R. M. Fleming, A. P. Ramirez, M. J. Rosseinsky, D. W. Murphy, R. C. Haddon, S. M. Zahurak and A. V. Mahija: *Nature* **352** (1991) 787.

31) T. Muramatsu, S. Yonezawa, Y. Muraoka and Z. Hiroi: *J. Phys. Soc. Jpn.* **73** (2004) 2912.

32) T. Muramatsu, N. Takeshita, C. Terakura, H. Takagi, S. Yonezawa, Y. Muraoka and Z. Hiroi: submitted to *Phys. Rev. Lett.*

33) R. Saniz, J. E. Medvedeva, L. H. Ye, T. Shishidou and A. J. Freeman: *Phys. Rev. B* **70** (2004) 100505.

34) H. Harima: in preparation.

35) A polycrystal of  $\text{LiTi}_2\text{O}_4$  was prepared by M. Isobe at ISSP.

36) O. Vyaselev, K. Kobayashi, K. Arai, J. Yamazaki, K. Kodama, M. Takigawa, M. Hanawa and Z. Hiroi: *J. Phys. Chem. Solids* **63** (2002) 1031.